



Article Processing Dates: Received on 2023-12-06, Reviewed on 2024-01-24, Revised on 2024-02-04, Accepted on 2024-04-03 and Available online on 2024-04-30

## Study of hydrodynamic characteristics in oscillating wave surge converter

James Julian<sup>1\*</sup>, Rizki Aldi Anggara<sup>1</sup>, Ridwan Daris Naufal<sup>1</sup>, Rifqi Ramadhani<sup>1</sup>, Eko Andi Prasetyo<sup>1</sup>, Fitri Wahyuni<sup>1</sup>, Nabilah Dwi Gunasti<sup>2</sup>

<sup>1</sup>Program Studi Teknik Mesin, Universitas Pembangunan Veteran Jakarta, Depok, 12450, Indonesia

<sup>2</sup>Program Studi Informatika, Universitas Pembangunan Veteran Jakarta, Depok, 12450, Indonesia

\*Corresponding author: zames@upnvj.ac.id

### Abstract

In the realm of renewable energy, researchers worldwide have been paying close attention to developing the Oscillating Wave Surge Converter (OWSC) device. This device has the potential to harness the power of ocean waves and convert it into a reliable source of clean energy. Hydrodynamic characteristics are essential parameters in developing OWSC devices. Therefore, this research conducted a hydrodynamic study on the OWSC device with variations in ocean wave periods, including  $T = 1.5, 1.7, 1.9, 2.1,$  and  $2.3$ . The Boundary Element Method (BEM) describes the interaction between sea waves and floating body structures. This method assumes incompressible, inviscid, and irrotational flow. A numerical approach is used as a calculation method followed by verification and validation to support the level of actualization. The research results showed that the incident wave caused the OWSC device to experience a deviation from its equilibrium position in the form of an oscillating flap inclination angle as a form of hydrodynamic characteristics. The sea wave period correlated with the rate of change in flap position over time, including the maximum deviation in the flap angle. As a power plant, the performance of the OWSC device can work at reasonably short-wave period intervals based on the device's ability to produce mechanical power. The highest average mechanical power was achieved in the  $T = 1.5$  period of 34.49 Watts with an efficiency of up to 52.43%. The OWSC device requires a high intensity of wave energy in a short duration to generate optimal mechanical power. It is important to note that optimal mechanical power generation is crucial for the OWSC device to function effectively. Therefore, the device should be placed in a location where the wave energy intensity is consistently high.

### Keywords:

OWSC, BEM, hydrodynamics, renewable energy, floating body.

### 1 Introduction

With increased human living standards, energy use in daily life is unavoidable [1]. Facts related to dependence on non-renewable energy are the main focus that needs to be considered when utilizing energy [2]. In addition, pollution and carbon emissions from fossil fuel consumption have become global climate challenges over the last few decades. Ocean wave energy is a promising renewable energy widespread worldwide, especially in Indonesia. As an archipelagic country, 70% of Indonesia's

territorial area comprises waters [3]. The seas in Indonesia have an enormous potential for sea wave energy, especially the waters that directly border the Indian Ocean, such as the waters that stretch from West Sumatra, South Java, to Nusa Tenggara [4]. Therefore, research related to the development of Wave Energy Converter (WEC) devices has become the focus of research on a global scale.

Since the 1970s, various research and developments related to WEC have been carried out [5]. Oyster and Wave Roller are Wave Energy Converter (WEC) technologies that have demonstrated the ability to operate effectively over extended periods [6], [7]. These devices are part of an Oscillating Wave Surge Converter (OWSC), which utilizes the movement of an inverted *pendulum* mechanism on a hinged plate on the seabed to capture ocean wave energy [8]. Comprehensive investigations related to OWSC are being conducted within the research's scope, covering various aspects. There's research that focuses on developing mathematical models to study the OWSC characteristics of waves [9]. The modeling results are further validated with available numerical and experimental data. OWSC is known to resonate due to the transverse sloshing modes of the channel. The computational solution is found in terms of a fast-converging series of Chebyshev polynomials of the second kind. The physical behavior of the system shows that the sensitivity of the resonant sloshing mode has a directly proportional relationship to the maximum efficiency. However, the ability of analytical methods is a limitation in comprehensively testing the characteristics of OWSC. Other research discusses the OWSC slamming phenomenon and its impact on the device [10]. The research was carried out experimentally and by 2D numerical simulation, with comparisons between the two to validate the numerical model. The study investigated the flow field, water surface evolution, and pressure distribution on the flap during a slamming event. From the calculation results obtained, slamming can significantly impact the performance and structural integrity of the OWSC. However, the limitation of the model is that it can only be described in a two-dimensional object so that the influence of the width of the *pendulum* plate is ignored. In addition, other research investigated four variations of the OWSC concept based on hydrodynamic response [11]. The power and flap rotation that occur as a result are determined using a model based on frequency domain analysis. The research results show that the four variations have different frequency dependencies. Apart from that, there is evidence of different values for the incident wave torque and the system's natural frequency.

To develop promising OWSCs, a comprehensive understanding of hydrodynamics is required. Building assumptions in developing new concepts is necessary for all technologies. However, building a concept on an OWSC that still needs to be mature causes many assumptions that need to be thoroughly reviewed, which ultimately causes the development of the concept to be inaccurate. Apart from that, the realization of OWSC technology development to date has been insignificant. Even though it is known as a technology with high efficiency, OWSC technology tends to require a large area of ocean wave effect to receive sufficient energy. In addition, varying marine environmental conditions narrow the operational scope of OWSC technology in utilizing ocean wave energy [12].

From a research world perspective, introducing assumptions built on validity is a critical factor in investigating the OWSC concept accurately and critically. Coupled with the limitations of OWSC technology, comprehensive testing regarding the characteristics of this technology has yet to be studied optimally [13]. Therefore, OWSC testing needs to be carried out further. This research focuses on the hydrodynamic characteristics of OWSC. Hydrodynamic characteristics are the primary basis for identifying the interaction of sea waves with electrical power

generation equipment. Tests were carried out with various wave periods to obtain a comprehensive and in-depth analysis. In addition, the performance efficiency of OWSC is reviewed based on the power generated from the device in the time domain model. By testing hydrodynamic characteristics, this research can be used as a specific guideline in determining parameter strategies for OWSC technology based on marine environmental conditions. Thus, OWSC technology can operate to utilize ocean wave energy to the maximum and with promising efficiency.

## 2 Research Methods

### 2.1 Ocean Waves Characteristics

In general, waves on the sea surface appear due to phenomena between various disturbing and restoring forces [14]. Wave Energy Converter (WEC) technology utilizes energy through waves formed by wind blowing on the sea surface [15]. As shown in Fig. 1, precisely, the wave particles move in a circular pattern with a gradient towards the water. However, the wave-particle movement pattern becomes more elliptical as the water depth decreases as a form of seabed effect [16]. Therefore, the characteristics of sea waves are classified into three different types, including 1) deep-water waves, which appear without the influence of a seabed and generally occur when the water depth is greater than half the wavelength; 2) shallow water waves, where there is no movement of wave particles varied ones that occur at water depths that are smaller than  $1/20^{\text{th}}$  of the wavelength; 3) transitional water waves that occur between two types of wave characteristics.

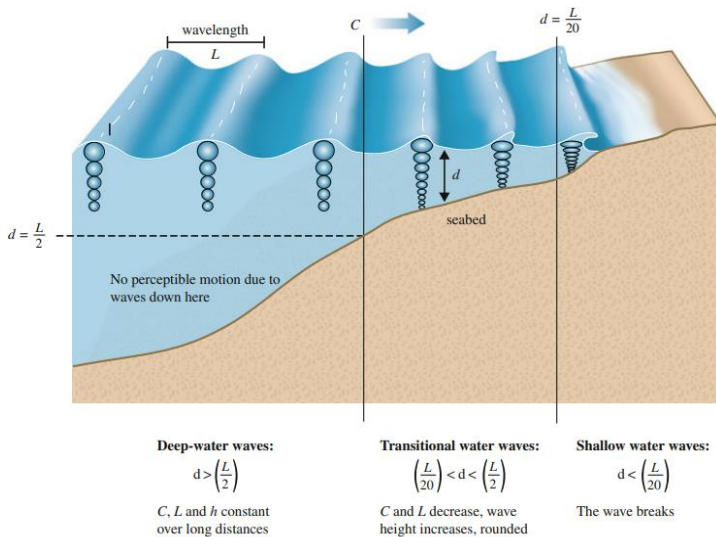


Fig. 1. Ocean waves characteristics [16].

### 2.2 Oscillating Wave Surge Converter (OWSC)

This research investigated the bottom-hinged plate as a type of Oscillating Wave Surge Converter (OWSC) model. In general, the bottom-hinged OWSC model is installed in the near shore region because the device was designed to extract energy from the horizontal motion of particles from sea waves. The interaction between waves and the seabed causes a shoaling effect, which the device utilizes. As a result, the movement of the wave particles, which were initially circular, becomes a horizontal elliptical shape. The OWSC model tested is a simplified concept of the OWSC model with a reduced scale of 40th based on research conducted by Wei [10]. Detailed geometric dimensions of the sample can be seen in Fig. 2.

### 2.3 Numerical Method

This research used a numerical approach to solve hydrodynamic cases in the study process. The Boundary Element Method (BEM) describes the interaction between sea waves and floating body structures [17]. This method assumes

incompressible, inviscid, and irrotational flow [18]. This research uses Ansys Aqwa hydrodynamic diffraction to solve hydrodynamic parameters, which includes two analysis methods, namely, frequency domain and time domain. In the time domain, the response of the WEC structure is analyzed in a dynamic scope to examine the hydrodynamic characteristics and performance [19].

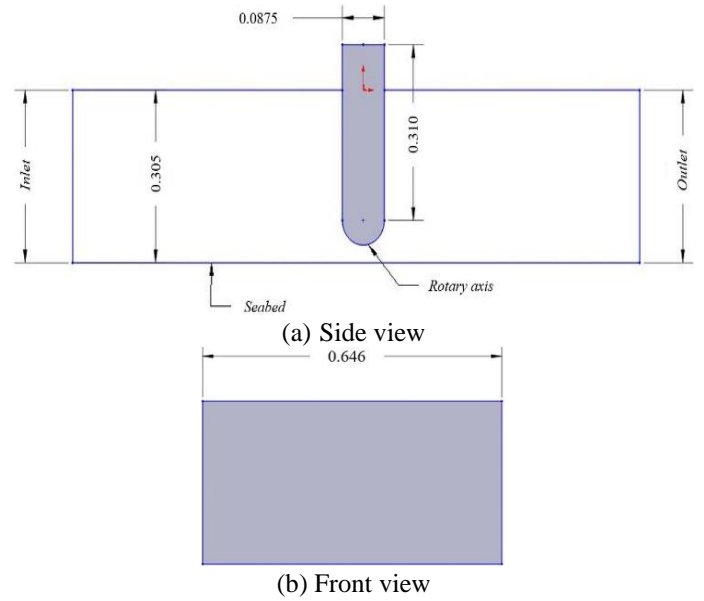


Fig. 2. Schematic of OWSC model dimensions.

This research used linear waves set out in Eq. 1 to model the ocean wave phenomenon. Ocean wave modeling varied in five different periods, as shown in Table 1. The wave force calculation uses the linear potential flow theory [20]. This theory is expressed through Eq. 2 as the velocity potential of the flow field. In addition, the time-averaged power wave on a period is defined in Eq. 3.

$$\eta(x, t) = \frac{H}{2} \cos(\omega t - k(x \cos \theta)) \quad (1)$$

$$\nabla^2 \phi(x, y, z, t) = \phi_I(x, y, z, t) + \phi_D(x, y, z, t) \quad (2)$$

$$+ \phi_R(x, y, z, t) = a_w \phi(x, y, z, t) e^{-i\omega t} \quad (3)$$

$$P_\omega = \frac{1}{2} \rho g A^2 c_g \quad (3)$$

$\eta(x, t)$	The surface elevation of a regular wave
$H$	The wave height
$\omega$	Angular velocity
$k$	Wave number
$\phi_I$	Incident wave velocity potential
$\phi_D$	The diffraction potential
$\phi_R$	The radiation potential
$P_\omega$	The time-averaged power
$\rho$	The fluid density
$A$	Wave amplitude
$g$	Gravity
$c_g$	Wave group velocity

Table 1. Parameters of waves

Period/s	Wave amplitude/m	Wavelength/m	Power/Watt
1.5	0.1	2.3572	65.792
1.7	0.1	2.73099	70.0303
1.9	0.1	3.0986	73.1444
2.1	0.1	3.46374	75.5343
2.3	0.1	3.8234	77.3195

In the OWSC performance testing process, the entire system can be applied in an equation [21]. Eq. 4 is the equation of the motion response in the OWSC system, which can be solved using a time domain solver through nonlinear hydrostatic and Froude-Krylov wave force calculations. The time domain solver involves hydrodynamic parameters in the form of coefficients obtained from the frequency domain solver [22]. The motion response output from OWSC in the frequency domain is written in Eq. 5.

$$M\ddot{X}(t) + C\dot{X}(t) + KX(t) + C_h\dot{X}(t) = F(t) \quad (4)$$

$$\left[ -\omega^2(M_s + M_a(\omega)) - i\omega C(\omega) + K \right] X(\omega) = F(\omega) \quad (5)$$

- $M$  The mass matrix
- $X(t)$  The displacement
- $C_h$  The damping of the hinge
- $C$  The damping matrix
- $F(t)$  Wave force
- $M_a$  The added mass matrix

## 2.4 Power Generated

The mechanical power output produced by the OWSC device could be investigated as a power plant. Mechanical power output is one of the primary considerations in considering the performance of OWSC devices. The *pendulum* flap is connected via a hinge to a fixed point, producing a moment as a mechanical response from the interaction between the device and sea waves. Mechanical power output is calculated by taking the absolute value of the product of damping moment and angular velocity, as shown in Eq. 6. In addition, this study tested the efficiency of the OWSC device. The efficiency of an OWSC device can be defined as the ratio between the time-averaged power wave and the average mechanical power set in Eq. 7.

$$P_{owsc} = |\tau(t) \cdot \omega(t)| \quad (6)$$

$$efficiency = \frac{\bar{P}_{owsc}}{P_\omega} \quad (7)$$

- $\tau$  Damping moment
- $\omega$  Angular velocity

## 2.5 Mesh Independence Study

A mesh independence study is needed to identify the mesh quality used in the computing process. Mesh independence study is a crucial stage in the numerical approach because it can affect the accuracy of the resulting data. Therefore, the mesh independence study was carried out based on the method applied in Roache's research [23]. This research tests mesh categories based on the number of elements, which include fine, medium, and coarse. Each mesh category's respective number of elements includes 18151, 9134, and 4563.

As a test sample, variable response oscillations on the flap were used for each mesh category, as in Fig. 3. Mesh testing was performed at wave specifications  $A = 0.1$  and  $T = 1.9$ . The image shows two graphs in a different domain, including the time and frequency domains. In each mesh category, the oscillation response curve in the time domain looks similar with minimal deviation. In the first period, the three curves show varying amplitudes until they finally start to stabilize at  $t > 15$ s. Therefore, further testing was conducted via Fast Fourier Transform (FFT) analysis.

This analysis is carried out to test variables in the frequency domain so that the dominant frequency acting on each curve can be determined. The specific FFT analysis results are in Table 2 as a comparison variable in the mesh independence study. After determining the test variables, each mesh category is identified

through the grid refinement ratio calculated in Eq. 6. Next, determine the order value through Eq. 7. In testing the error value for each mesh category, the Grid Convergence Index (GCI) calculated in Eq. 8 and Eq. 9 is used as a parameter. GCI is divided into two categories:  $GCI_{fine}$  as the error value between fine and medium mesh and  $GCI_{coarse}$  as the error value between medium and coarse mesh.

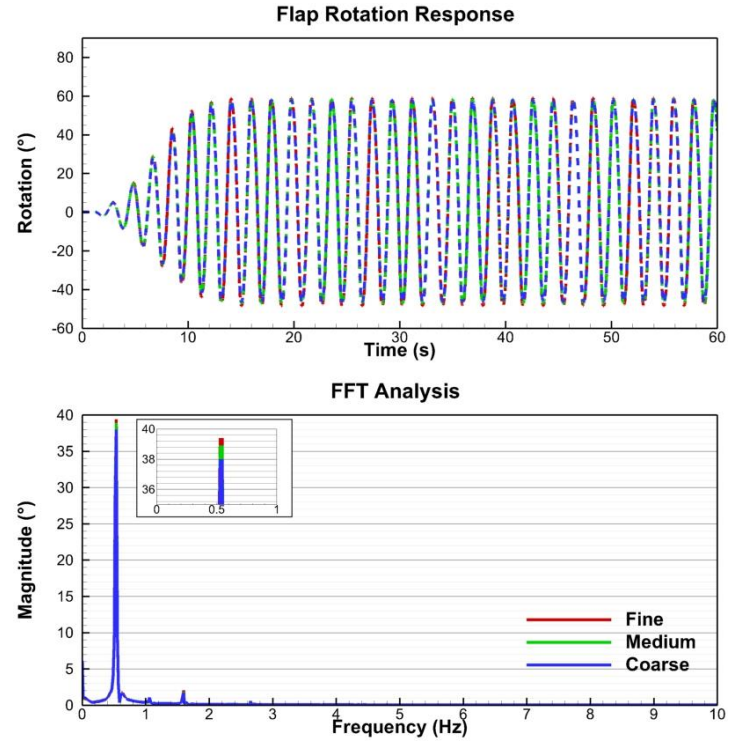


Fig. 3. OWSC rotation response ( $^\circ$ ) per unit-time (s).

Table 2. FFT results

Mesh category	Magnitude ( $^\circ$ )	Frequency (Hz)
Fine	39.40	0.5380
Medium	38.90	0.5380
Coarse	38.00	0.5380

$$r = \frac{h_2}{h_1} \quad (6)$$

$$p = \frac{\ln\left(\frac{f_3 - f_2}{f_2 - f_1}\right)}{\ln(r)} \quad (7)$$

$$GCI_{fine} = \frac{F_s |\epsilon|}{(r^p - 1)} \quad (8)$$

$$GCI_{coarse} = \frac{F_s |\epsilon| r^p}{(r^p - 1)} \quad (9)$$

$$\epsilon = \frac{f_{n+1} - f_n}{f_n} \quad (10)$$

$$\frac{GCI_{coarse}}{GCI_{fine} r^p} \approx 1 \quad (11)$$

$$f_{r_{h=0}} = f_1 + \frac{(f_1 - f_2)}{(r^p - 1)} \quad (12)$$

To ensure the error value for each mesh is correct, the GCI calculation must be in the convergence area. Therefore, the actual value of the mesh independence study can be obtained in Eq. 12.

The results of the mesh independence study can be seen in Table 3. The test results show that the fine mesh has guaranteed accuracy with the smallest error value. Therefore, a fine mesh was chosen for the test's mesh setup.

Table 3. Mesh independence test result

Mesh	Fine	Medium	Coarse
Velocity	39.40	38.90	38.00
$r$		0.847996907	
$GCI_{\text{fine}}$		2	
$GCI_{\text{coarse}}$		2.008%	
		3.6150%	
		40.025	
		1	
Error	1.56152%	2.81074%	5.05934%

### 3 Results and Discussion

#### 3.1 Validation

Validation is an essential stage in numerical calculation due to the approach method used. It is needed to ensure the level of actualization of the calculation results obtained. The OWSC device investigated in this study will be validated with experimental research data conducted by Wei [10]. The motion response data of the OWSC device due to ocean wave events is used for the comparison process with experimental data. The motion data response of the OWSC device was taken on ocean waves with specifications  $A = 0.1$  and  $T = 1.9$ . The motion response of the OWSC device due to sea waves can be seen in Fig. 4. Based on the calculation results, Fig. 4 shows the OWSC device's resonance results with sea waves similar to experimental data. The motion response of the OWSC device forms an isolated sinusoidal wave curve following the wave period, even though there is a slight difference in the maximum tilt angle produced between the numerical data and the experimental data. However, the calculation results show a level of validity that is good enough to fulfill actual conditions. In addition, by calculating the phase

difference using the Fourier model, it was found that the phase error between the simulation data and the experiment was 8%.

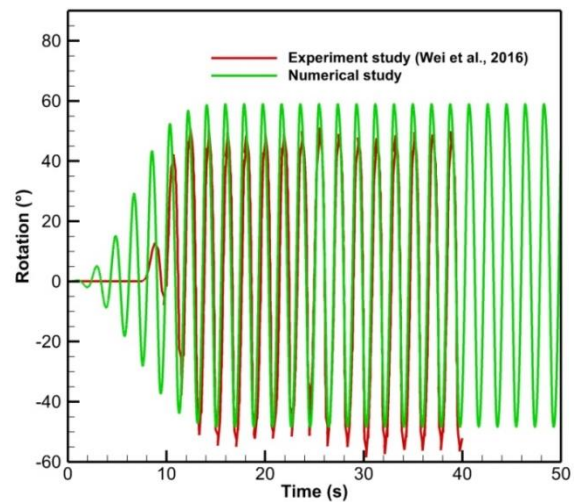


Fig. 4. OWSC rotation response (°) per unit-time (s).

#### 3.2 Analysis

This research aimed to examine the hydrodynamic properties and efficiency of the OWSC device. Tests were carried out with a variety of different wave periods. In Fig. 5, the response of the OWSC device for each different wave period is shown. The characteristics of the OWSC device show resonance in the form of oscillatory motion with sea waves at each period. The flap moves as an inverted *pendulum* that is hinged to the seabed. Ocean wave incidents cause the flap to deviate from its equilibrium position with changes in the tilt angle per unit of time. In addition, there is a slight change in the maximum tilt angle produced on each flap, followed by the received wave intensity. Based on the results of calculations, the response produced by the OWSC device shows quite good stability. The flap movement response stabilizes when the travel time is  $t > 15$ . Furthermore, no significant changes in the device's response disrupt its stability.

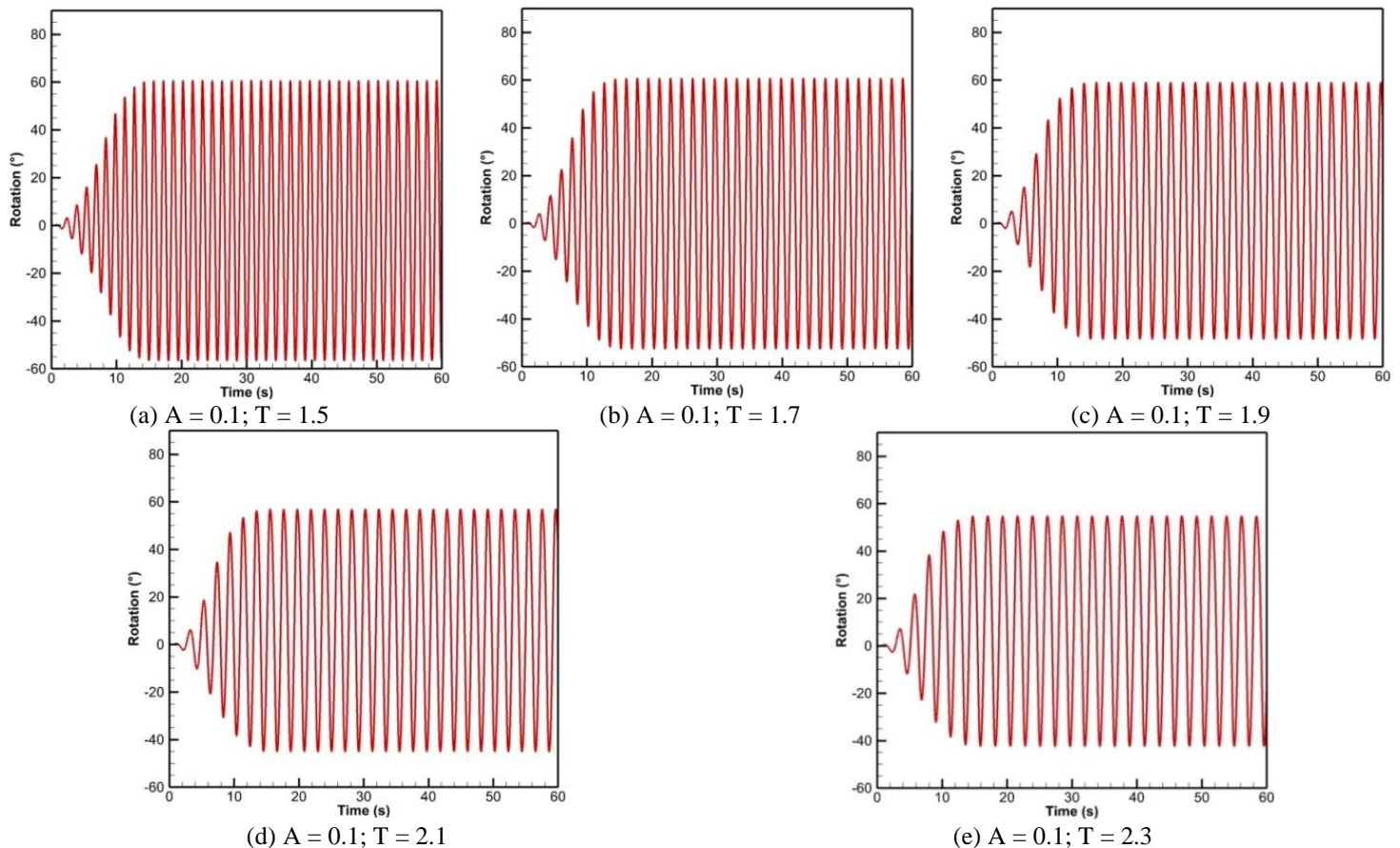


Fig. 5. OWSC rotation response (°) per unit time (s).

More specifically, the change in inclination angle position phenomenon experienced by the flap on the OWSC device is reviewed in more depth. Fig. 6 shows the correlation between angular velocity, damping moment, and power. Based on the response phenomenon shown on the OWSC device, every change in phase angle experienced by the flap shows a different condition. At the equilibrium position, the incoming sea waves cause the flap to accelerate in one direction until it reaches maximum angular velocity. When reaching maximum angular velocity, the flap experiences deceleration due to various factors, including buoyancy force, which meets Archimedes' law and hydrostatic pressure principles. This condition continues until the flap shows the maximum inclination angle and experiences acceleration due to incident sea waves in the opposite direction.

In addition, Fig. 6 shows the influence of sea wave events on the resulting damping moment. The oscillatory motion of the flap shows characteristics at each angle condition. The damping moment that can be produced creates a phase difference relationship on an angular velocity curve. The curves of the two variables show different phases up to  $180^\circ$  so that the magnitude of each variable shows a different vector direction. The correlation of the resulting damping moment with angular velocity is related to variable power. The results show that power is an absolute

value of the product between damping moment and angular velocity. Therefore, the  $180^\circ$  phase difference relationship in angular velocity and damping moment provides favorable behavior so that the maximum power that the OWSC device can produce is under conditions where the angular velocity and damping moment are maximum. Based on the calculation results, the sea wave period significantly influences the movement cycle rate of the OWSC device. The gradient response of the device is represented as the change in angular velocity produced by the OWSC device followed by the wave period. The sea wave period influences two essential parameters on the response of the OWSC device, which include the rate of change and maximum value. In Fig. 6, the wave period  $T = 1.5$  shows that the two parameters indicate the maximum conditions for the form of interaction of the OWSC device with sea waves. Therefore, the OWSC device can produce maximum power. The ability of OWSC devices to generate power decreased following a period of sea wave growth. This condition is indicated in the rate of change and maximum value of the angular velocity and damping moment variables. Thus, the power generation performance of the OWSC device shows maximum conditions when it is in the low wave period and experiences a significant decline followed by a period of increase.

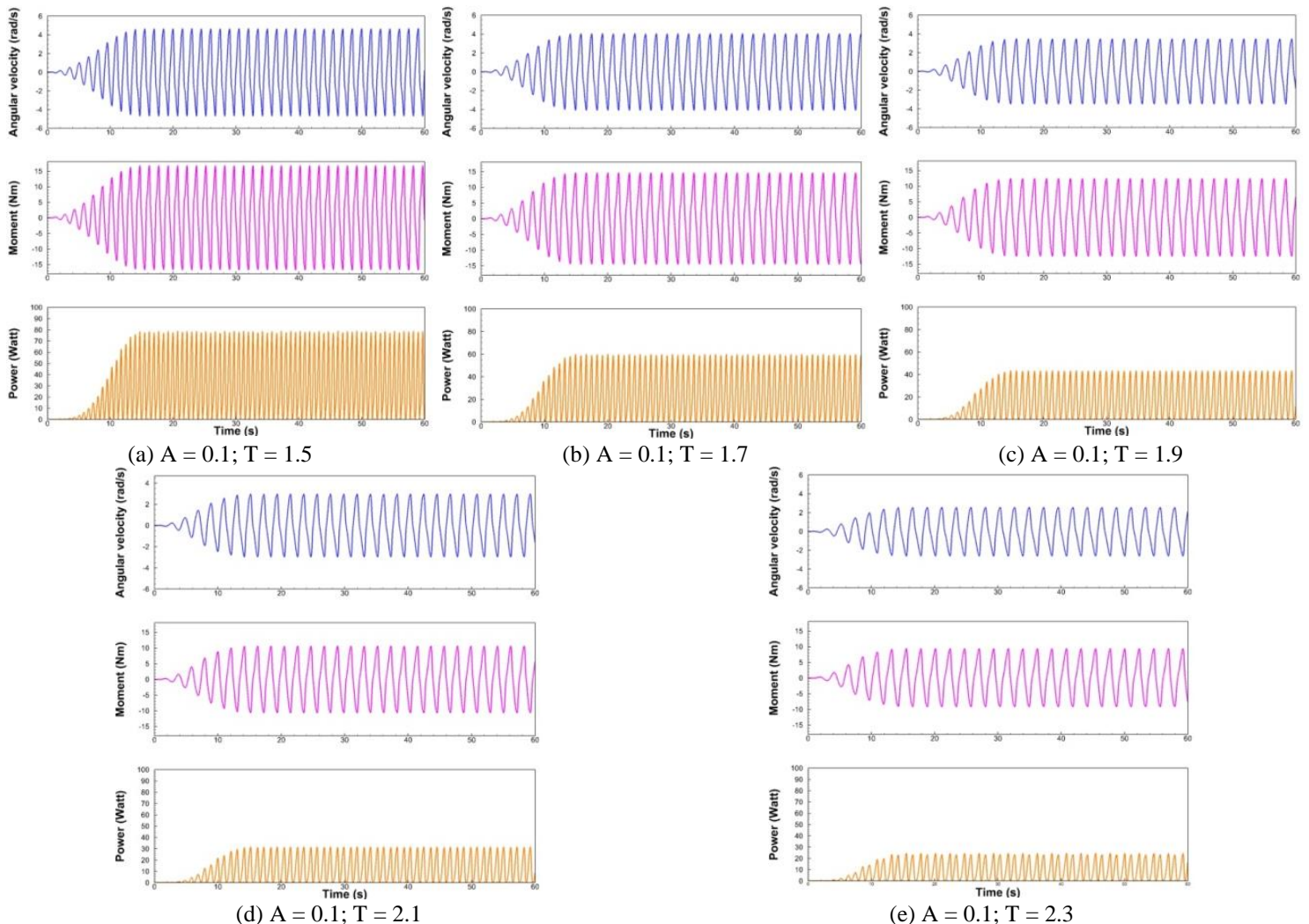


Fig. 6. Angular velocity (rad/s), damping moment (Nm), and power (Watt) generated of OWSC per unit time (s).

In addition, the relationship between ocean wave power and average mechanical power is shown in Fig. 7. Ocean wave power is a parameter that is the ability of a medium to carry energy at a rate of change over some time. Period shows the duration required to produce one wave cycle. Period changes to the power produced by ocean waves have a directly proportional relationship. Periods with a longer duration have a wave size or length that is large

enough to increase the wave's ability to carry resultant energy. However, the calculation results show that the OWSC device has an inverse relationship in the average mechanical power variable to ocean wave power. Increasing the sea wave period causes a significant decrease in the average mechanical power produced.

A mismatch between the characteristics of the device mechanism and the characteristics of ocean waves indicates a

decrease in the performance of the OWSC device. In addition, the performance of OWSC is contrary to the findings of investigations in research conducted by QiaofengLi *et al.*, 2021 [24]. In this research, the self-floating Oscillating Surge Wave Converter (floating-OSWC) type technology showed an upward trend in mechanical power in the same period interval. The significant differences in the submerged-OWSC type indicate that differences in hydrodynamic characteristics influence the extraction power of sea wave energy. The OWSC device performed well in producing average mechanical power during high-wave periods. The efficiency of the OWSC device is also reviewed in Table 4 in more detail. At peak performance, the OWSC device can achieve an efficiency of up to 52.43% in the  $T = 1.5$  wave period. A significant decrease in efficiency occurred, followed by a decrease in the performance of the device producing mechanical power until the lowest efficiency was achieved, up to 13.48% in the  $T = 2.3$  wave period. A significant decrease in efficiency shows the energy dissipated in the device. OWSC devices have limitations in maintaining efficiency in their performance in relatively low wave period areas. The intensity of the number of waves in a unit of time must be met to improve the performance of the OWSC device through wave kinetic energy. Therefore, the rate of rotation change produced by the device increases, followed by increased mechanical power.

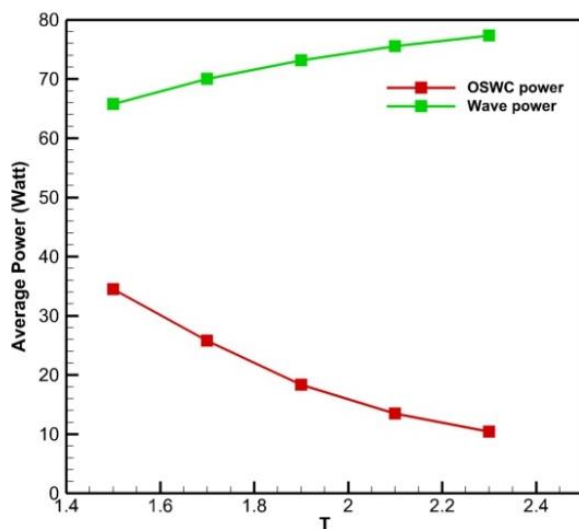


Fig. 7. Average power output of OWSC vs wave power.

Table 4. Efficiency of OWSC

Period/s	Efficiency
1.5	52.43%
1.7	36.79%
1.9	25.04%
2.1	17.88%
2.3	13.48%

#### 4 Conclusion

Hydrodynamic testing on the OWSC device was carried out in this research using a numerical approach with a time domain model. A comprehensive analysis was conducted by varying sea wave periods and validating data. Testing was conducted to obtain the hydrodynamic characteristics and performance of the OWSC device as a power generator. The research results show that the OWSC device is a form of inverted *pendulum* mechanism where the flap is hinged on the seabed. The incoming wave causes the device to experience a deviation from the specified position in the form of a flap tilt angle, which drives oscillations as a form of hydrodynamic characteristics. The sea wave period correlated with the rate of change in flap position with time. The sea wave period also influences the maximum deviation in the flap angle, so the value of the resulting damping moment is very influential. The

oscillatory motion of the OWSC device is capable of resonating at any variation in the period of ocean waves. Therefore, the shortest sea wave period shows the most significant rate of change and deviation, especially in the period  $T = 1.5$ . In addition, this condition is directly proportional to the angular velocity and damping moment produced.

As a power plant, the mechanical power significantly produced determines the performance of the OWSC device being tested. The calculation results show that the OWSC device requires quite a lot of wave intensity to obtain high mechanical power. The sea wave period dramatically affects the performance of the OWSC device. The peak performance of the OWSC device was obtained in the shortest wave period with  $T = 1.5$ , with an average mechanical power produced of more than 30 Watts, followed by an efficiency of up to 52.43%. However, increasing the wave period causes a decrease in the performance of the OWSC device until the average mechanical power is reached at 10.42 Watts. In addition, the inability of the OWSC device to capture considerable ocean wave energy during high periods causes a significant decrease in efficiency of up to 13.48%. The OWSC devices have limited capabilities when it comes to short-wave periods.

#### References

- [1] F. Junejo, A. Saeed, and S. Hameed, "5.19 Energy Management in Ocean Energy Systems," in *Comprehensive Energy Systems*, I. Dincer, Ed., Oxford: Elsevier, 2018, pp. 778–807. doi: <https://doi.org/10.1016/B978-0-12-809597-3.00539-3>.
- [2] M. Azhar and D. Satriawan, "Implementasi Kebijakan Energi Baruan Energi Terbarukan Dalam Rangka Ketahanan Energi Nasional," *Administrative Law and Governance Journal*, vol. 1, pp. 398–412, Nov. 2018, doi: 10.14710/alj.v1i4.398-412.
- [3] R. Kurniawan, M. Habibie, and D. Permana, "KAJIAN DAERAH RAWAN GELOMBANG TINGGI DI PERAIRAN INDONESIA (STUDY ON HIGH WAVE PRONE AREAS OVER INDONESIAN WATERS)," Dec. 2012, doi: 10.31172/jmg.v13i3.135.
- [4] I. U. N. Rais and S. Hastuti, "Analisis Pengaruh Lebar Kolom Osilasi Pembangkit Listrik Tenaga Gelombang Laut Tipe Oscillating Water Column (OWC) Terhadap Daya yang Mampu Dibangkitkan di Wilayah Kelautan Indonesia," 2018.
- [5] A. F. de O. Falcao, "Wave energy utilization: A review of the technologies," *Renewable and sustainable energy reviews*, vol. 14, no. 3, pp. 899–918, 2010.
- [6] E. Renzi, K. Doherty, A. Henry, and F. Dias, "How does Oyster work? The simple interpretation of Oyster mathematics," *European Journal of Mechanics-B/Fluids*, vol. 47, pp. 124–131, 2014.
- [7] T. Whittaker and M. Folley, "Nearshore oscillating wave surge converters and the development of Oyster," *Philosophical Transactions of the Royal Society A: Mathematical, Physical and Engineering Sciences*, vol. 370, no. 1959, pp. 345–364, 2012.
- [8] Y. Cheng, L. Tang, and C. Ji, "Three-dimensional hydrodynamic analysis and efficiency optimization of submerged multi-cylindrical oscillating wave surge converter," *Ocean Engineering*, vol. 215, p. 107710, 2020.
- [9] E. Renzi and F. Dias, "Resonant behaviour of an oscillating wave energy converter in a channel," *J Fluid Mech*, vol. 701, pp. 482–510, 2012.
- [10] Y. Wei, T. Abadie, A. Henry, and F. Dias, "Wave interaction with an oscillating wave surge converter. Part II: Slamming," *Ocean Engineering*, vol. 113, pp. 319–334, 2016.
- [11] S. Gunawardane, M. Folley, and C. J. Kankanamge, "Analysis of the hydrodynamics of four different oscillating

- wave surge converter concepts,” *Renew Energy*, vol. 130, pp. 843–852, 2019.
- [12] M. J. Khatibani and M. J. Ketabdari, “Numerical modeling of an innovative hybrid wind turbine and WEC systems performance: A case study in the Persian Gulf,” *Journal of Ocean Engineering and Science*, 2022, doi: <https://doi.org/10.1016/j.joes.2022.05.008>.
- [13] S. Foteinis and T. Tsoutsos, “Strategies to improve sustainability and offset the initial high capital expenditure of wave energy converters (WECs),” *Renewable and Sustainable Energy Reviews*, vol. 70, pp. 775–785, 2017, doi: <https://doi.org/10.1016/j.rser.2016.11.258>.
- [14] O. Farrok, *Oceanic Wave Energy Conversion: Advancement of Electrical Generators*. Springer Nature.
- [15] X. Zhao et al., “Hydrodynamic analysis of a floating platform coupled with an array of oscillating bodies,” *Ocean Engineering*, vol. 287, p. 115439, 2023, doi: <https://doi.org/10.1016/j.oceaneng.2023.115439>.
- [16] T. Garrison, *Oceanography: An Invitation to Marine Science*. National Geographic Learning, Brooks/Cole, Cengage Learning, 2013.[Online]. Available: <https://books.google.co.id/books?id=1qyBtgAACAAJ>
- [17] J. N. Newman, *Marine hydrodynamics*. The MIT press, 2018.
- [18] B. Bosma, T. Brekken, H. Ozkan-Haller, and S. Yim, *Wave energy converter modeling in the time domain: A design guide*. 2013. doi: 10.1109/SusTech.2013.6617305.
- [19] W. Tongphong, B.-H.Kim, I.-C.Kim, and Y.-H. Lee, “A study on the design and performance of ModuleRaft wave energy converter,” *Renew Energy*, vol. 163, pp. 649–673, 2021.
- [20] M. Rahman, “Water waves: relating modern theory to advanced engineering applications,” 1995.
- [21] O. Faltinsen, *Sea loads on ships and offshore structures*, vol. 1. Cambridge university press, 1993.
- [22] Y. Lin and F. Pei, “Numerical study on bottom-hinged plate wave energy converter geometry design,” *Ocean Engineering*, vol. 260, p. 112050, 2022.
- [23] P. J. Roache, “Perspective: a method for uniform reporting of grid refinement studies,” 1994.
- [24] Q. Li, J. Mi, X. Li, S. Chen, B. Jiang, and L. Zuo, “A self-floating oscillating surge wave energy converter,” *Energy*, vol. 230, p. 120668, 2021.